Structural Engineering and Mechanics, *Vol. 58, No. 4 (2016) 731-743*
DOI: http://dx.doi.org/10.12989/sem.2016.58.4.731

Plastic behavior of circular discs with temperature-dependent properties containing an elastic inclusion

Somayeh Bagherinejad Zarandi[1], Yun-Che Wang[*1] and Olga V. Novozhilova[2]

[1]*Department of Civil Engineering, National Cheng Kung University, 1 University Road, Tainan, 70101, Taiwan*
[2]*Bauman Moscow State Technical University, 2nd Baumanskay street 5, 105005, Moscow, Russia*

(Received October 3, 2015, Revised December 15, 2015, Accepted January 15, 2016)

Abstract. Plastic behaviors, based on the von Mises yield criterion, of circular discs containing a purely elastic, circular inclusion under uniform temperature loading are studied with the finite element analysis. Temperature-dependent mechanical properties are considered for the matrix material only. In addition to analyzing the plane stress and plane strain disc, a 3D thin disc and cylinder are also analyzed to compare the plane problems. We determined the elastic irreversible temperature and global plastic collapse temperature by the finite element calculations for the plane and 3D problem. In addition to the global plastic collapse, for the elastically hard case, the plane stress problem and 3D thin disc may exhibit a local plastic collapse, i.e. significant pile up along the thickness direction, near the inclusion-matrix interface. The pileup cannot be correctly modeled by the plane stress analysis. Furthermore, due to numerical difficulties originated from large deformation, only the lower bound of global plastic collapse temperature of the plane stress problem can be identified. Without considerations of temperature-dependent mechanical properties, the von Mises stress in the matrix would be largely overestimated.

Keywords: plasticity; finite element analysis; temperature-dependent material properties; composite circular disc; elastic inclusion

1. Introduction

The in-plane behaviors of discs with temperature-dependent properties under thermal loading have attracted much attention in the past years due to their scientific and industrial importance (Argeso and Eraslan 2008, Alexandrov *et al.* 2014, Alexandrov *et al.* 2014). Although the plasticity problems of solid or annular discs with temperature-independent mechanical properties, based on the plane strain or plane stress assumption, have long been studied under various types of loading conditions (Lubliner 1990), recent analytical results on the discs under thermal loading have shed new light along this line of research (Alexandrov and Alexandrova 2001, Alexandrov and Chikanova 2000, Alexandrov *et al.* 2012). In particular, analytical solutions for the plane-stress problem of the composite disc with temperature-dependent mechanical properties are still lacking, even though effects of temperature-dependent properties have long been recognized (Noda 1991). In addition, effects of thickness variations on the elastoplastic behavior of annular discs have been

*Corresponding author, Associate Professor, E-mail: yunche@mail.ncku.edu.tw

http://www.techno-press.org/?journal=sem&subpage=8 ISSN: 1225-4568 (Print), 1598-6217 (Online)

studied (Wang *et al.* 2013). As for material's capability to dissipate energy done by external load, Wang and Ko (2015) reported the energy dissipation properties of a composite beam-column connector due to viscoelastic and plastic deformation processes.

For the plasticity problems of the composite disc, Guven (1997), Guven and Altay (1998) studied rotating discs for the rigid inclusion case with the analytical approach. Furthermore, The elastic-plastic problems of the rotating disc with rigid inclusion have also been alanyzed (Parmaksizoglu and Guven 1998). Eraslan and Akis (2003) studied the elastic-plastic deformation of a rotating disk subjected to radial temperature gradient. Aluminum composite discs under thermal loading have been studied (Altan *et al.* 2008, Topcu *et al.* 2008). In addition, under temperature effects, shrink fit problems with solid inclusion have been investigated (Bengeri and Mack 1994, Mack and Bengeri 1994, Mack and Plochl 2000). Ball (1995) studied the elastic-plastic problem of fastener holes under cold expansion. None of the above studies consider temperature-dependent mechanical properties. In addition, the composite disc problem is related to functionally graded materials problem since the composite disc represents a special type of distributions of mechanical properties in terms of space coordinates (Krenev *et al.* 2015, Kwon *et al.* 1994, Lutz *et al.* 1996, Reddy and Chin 1998).

Comparisons between the finite element analysis and experiment have been performed and reasonable agreements have been verified (Luxmoore *et al.* 1977, Sayman and Arman 2006). It is known that the plane stress elastoplastic problems may encounter numerical difficulties (Jetteur 1986, Kleiber and Kowalczyk 1996, Triantafyllou and Koumousis 2012, Valoroso and Rosati 2009, Simo and Taylor 1986). In this work, we adopt the mature finite element method to numerically study the plastic behavior of the composite disc in two and three dimensions to serve as reference data for future analytical solutions on such problem.

2. Theoretical and numerical aspects

The problem statement of the mechanics problem studied here is as follows. A purely elastic inclusion is embedded in an elastoplastic, circular matrix to form the concentric, composite disc. The outer rim of the composite disc is mechanically fixed (i.e., clamped), and a uniform temperature difference is statically applied to the whole disc, as the thermal loading. No dynamics or thermal diffusion is considered here. The physical properties of the purely elastic inclusion are assumed to be temperature independent, but those of the elastoplastic matrix are temperature dependent (mainly the yield stress temperature dependence). The 2D problems, including the plane-stress and plane-strain problems, and the 3D problems, including a cylinder and thin plate, are numerically solved to investigate their plastic behaviors. For the 3D cylinder case, the outer circumferential surface is fixed along the three orthogonal coordinates, as well as the top and bottom flat surface. For the 3D disc case, only the outer circumferential surface is fixed along the three orthogonal coordinates. For the plane stress case, the fixed boundary condition on the outer rim only provides constraints along the two orthogonal coordinates, while the plane strain case requires zero displacements on the outer rim along all three orthogonal coordinates. Both of the 3D cases are numerically solved with the axisymmetric assumption. The inclusion-matrix interface is assumed to be perfectly bonded.

Finite element analysis was conducted here to investigate the abovementioned 2D and 3D problems. Changing the thickness of the 3D models may 'force' them behave like the plane-stress or plane strain problem. In other words, the 3D cylinder may behave similar to the plane strain disc when the cross section of the cylinder is far away from its ends. The 3D thin plate, termed as the 3D disc in this work, may not behave like the 2D plane stress disc, due to deformation and stress along the *z* direction being different in the inclusion and matrix, which are not explicitly analysed in the plane problem. Boundary conditions used in the plane-stress case and 3D disc case are different. The displacements along three orthogonal coordinates are set to zero at the outer rim of the 3D disc, while only two in-plane displacements are set to be zero for the plane stress case. One of the aims of the paper is to numerically demonstrate the similarities and differences among the four problems, i.e., the plane stress, plane strain, 3D disc and 3D cylinder problem, with the chosen boundary conditions.

The three-dimensional von Mises criterion requires stresses (σ_{ij}) satisfy the following equation with the tensile yield stress σ_y on the yield surface (Lubliner 1990).

$$F = \sigma_{mises} - \sigma_y = 0 \tag{1}$$

where the yield function is denoted by *F*, and the von Mises stress is defined as follows in terms of deviatoric stress tensor s_{ij}, or its second invariant.

$$\sigma_{mises} = \sqrt{3J_2(s_{ij})} = \sqrt{\frac{3}{2}s_{ij}s_{ij}} \tag{2}$$

$$s_{ij} = \sigma_{ij} - \frac{1}{3}\sigma_{kk}\delta_{ij}s_{ij} \tag{3}$$

Here δ_{ij} is the Kronector delta function, and the Einstein summation rule for the indices is applied. For the 2D plane-stress problem above yield condition can be expressed in terms of the radial and hoop stress, as follows.

$$\sigma_r^2 + \sigma_\theta^2 - \sigma_\theta\sigma_r = \sigma_y^2 \tag{4}$$

Local effective plastic strain can be obtained from plastic strain by

$$\dot{\varepsilon}_{pe} = \sqrt{\frac{2}{3}\dot{\varepsilon}_{ij}^p\dot{\varepsilon}_{ij}^p} \tag{5}$$

and the energy dissipation density due to plastic deformation is calculated as follows.

$$D_p = \sigma_{ij}\dot{\varepsilon}_{ij}^p \tag{6}$$

Our finite element models are shown in Fig. 1. A specific geometry with the inner radius a_0=0.3 m and outer radius b_0=1 m is studied, where the subscript 0 indicates the undeformed state of the composite disc. The thickness of the 3D disc, as shown in Fig. 1(b), is 0.1 m, and the length of the 3D cylinder, as shown in Fig. 1(c), is 10 m. In other words, the aspect ratio between thickness (or length) and radius is 10 for the 3D disc (or 3D cylinder).

In Figs. 1 (b) and (c), the color indicates the mesh size distribution. For the 3D disc, mesh size is distributed between 0.00675 and 0.0112 m among the colors, and for the 3D cylinder, mesh size between 0.0788 and 0.109 m. Smaller mesh size, compared to the dimensions of the model, ensures numerical accuracy. Since the 3D problems are solved based on the axisymmetric assumption, there are about 2600 triangular quadratic elements, and about 66000 numbers of

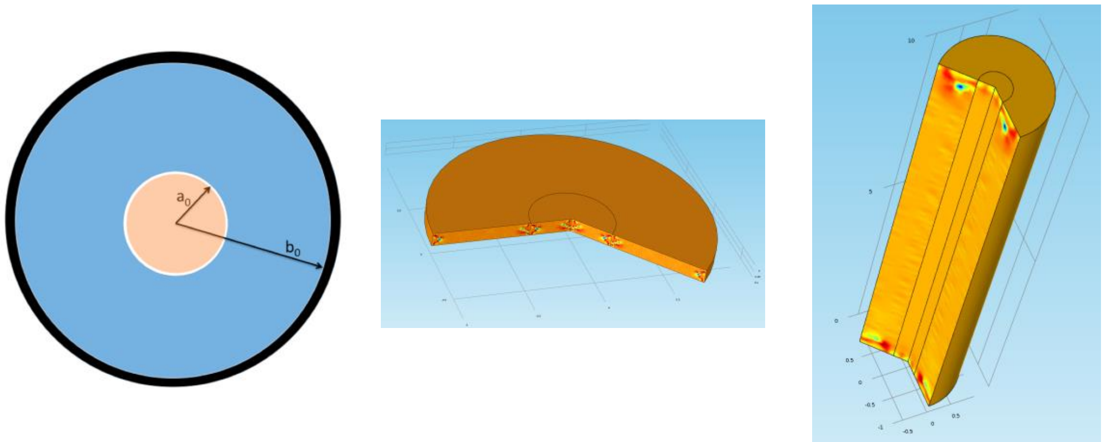

(a) 2D disc (b) 3D disc (c) 3D cylinder

Fig. 1 Models that are analyzed in this work

degrees of freedom (D.O.F.), with additional about 220000 internal D.O.F. for plasticity, used in the calculations. For 2D problems, about 22000 triangular quadratic elements, and about 90000 numbers of degrees of freedom (with additional about 600000 internal D.O.F. for plasticity) were used in the calculations. We deliberately chose different number of elements in the 2D and 3D cases to test their numerical accuracies. In all of the models, the interface between inclusion and matrix is assumed to be perfectly bonded in this study.

Our finite element calculations were performed with COMSOL (2015), which follows the algorithm proposed by Simo and Taylor (1986) to solve the plasticity problem. The implicit static solver, multifrontal massively parallel solver (MUMPS), was chosen to solve algebraic equation systems.

As for the temperature-dependent material properties of the matrix, we assume it is an elastic-perfectly plastic isotropic, homogeneous material with temperature-dependent properties. As suggested by Aegeso and Eraslan (2008), the dimensionless, temperature functions, $f_\sigma(\Delta T)$, $f_E(\Delta T)$, $f_\nu(\Delta T)$ and $f_\gamma(\Delta T)$, for a high-strength low-alloy steel the temperature difference is in the range $0 \le T < 400$℃ can be expressed as follows. Here the subscripts σ, E, ν and γ denote yield stress, Young's modulus, Poisson's ratio and linear thermal expansion coefficient, respectively. The below four functions are dimensionless quantities since the numeric coefficients contain units to cancel units from the ΔT or ΔT^2 terms.

$$f_\sigma(\Delta T) = 1 + \frac{\Delta T}{600 \ln(\Delta T / 1630)} \tag{7}$$

$$f_E(\Delta T) = 1 + \frac{\Delta T}{2000 \ln(\Delta T / 1100)} \tag{8}$$

$$f_\nu(\Delta T) = 1 + 2.5 \times 10^{-4} \Delta T - 2.5 \times 10^{-7} \Delta T^2 \tag{9}$$

$$f_\gamma(\Delta T) = 1 + 2.56 \times 10^{-4} \Delta T - 2.14 \times 10^{-7} \Delta T^2 \tag{10}$$

where the temperature difference ΔT is in °C and it is the difference between processing temperature and the reference (i.e., room) temperature which is 20°C. Also, at the reference temperature, the Young's modulus, yield stress, Poisson's ratio and linear thermal expansion coefficient of the matrix material are assumed to be E_0=200 GPa, σ_0=410 MPa, ν_0=0.3, and $\gamma_0=11.7\times10^{-6}$ per °C, respectively. Hence, the Young's modulus $E_m(\Delta T)=E_0\ f_E(\Delta T)$, $\sigma_m(\Delta T)=\sigma_0\ f_\sigma(\Delta T)$, $\nu_m(\Delta T)=\nu_0\ f_\nu(\Delta T)$, $\gamma_m(\Delta T)=\gamma_0\ f_\gamma(\Delta T)$ for the matrix, indicated by subscript m. For the purely elastic inclusion, indicated by subscript *i*, all of its material properties are temperature independent, and we assume the inclusion Young's modulus $E_i=\lambda E_{i0}$, the inclusion Poisson's ratio ν_i=0.28, the inclusion linear thermal expansion coefficient $\gamma_i=\lambda\ \gamma_{i0}$. The reference Young's modulus and linear thermal expansion coefficient of the inclusion are 411×10^9 Pa and 50×10^{-6} per °C, evalues were chosen to represent a ceramic material for the inclusion. Note that changing λ would affect both Young's modulus and thermal expansion simultaneously. As for the density of the two materials, ρ_m=7900 for the steel matrix and ρ_i=5000 kg/m^3 for the ceramic inclusion were chosen. It is noted that the densities may also be function of temperature, but in the present analysis we assume they are constant. Since it is impossible to set the inclusion to be rigid in the finite element calculations, it is needed to numerically test if the chosen inclusion's yield strength is large enough to avoid any plasticity. In this study, we have verified that the inclusion is not yielded in the all the cases studied here.

3. Results and discussion

3.1 Temperature-dependent material properties

Fig. 2 shows the dimensionless, temperature dependent functions for the yield stress, Young's modulus, Poisson's ratio and linear thermal expansion coefficient. It can be seen that the Poisson's

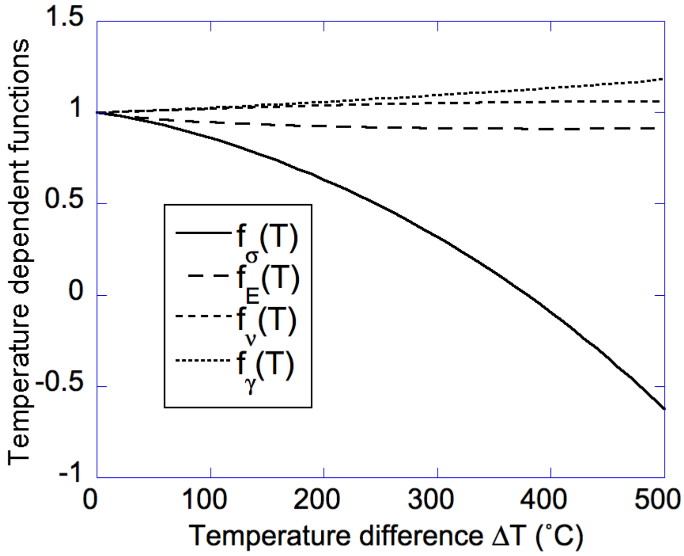

Fig. 2 Temperature-dependent functions to describe the changes of the material properties with temperature

ratio and thermal expansion coefficient are monotonically increasing functions with small slopes. Young's modulus is a slightly decreasing function. Only the yield stress shows strong temperature dependence, Hence, in this work, we only report the effects of the yield stress temperature dependence. It is observed in many cases that the involvement of other temperature dependent functions do not significantly alter the results reported here.

3.2 Two-dimensional analysis–plane strain

For λ=10, i.e., E_i/E_0=20.55 and γ_i/γ_0=42.7, the von Mises stress distribution along the radius in the plane strain circular disc under various uniform temperature loading is shown in Fig. 3(a). Since $E_i > E_0$, the inclusion is an elastically harder phase than the matrix at the reference temperature. In addition, the inclusion has more thermal expansion because of a larger γ_i. It can be seen that when ΔT=20℃, the matrix is fully plastically yielded. Hence, the global plastic collapse temperature for the disc is ΔT_p=20℃. It is noted that ΔT_p is a function of mechanical properties of the disc and its geometry. Furthermore, the disc exhibits the elastic irreversible temperature ΔT_e, defined as initial yield occurs in the matrix, is about 1.5℃ (determined by finer parametric analysis, not shown in the figure). The spatial distribution of the von Mises stress in the disc when ΔT=20℃ is shown in Fig. 3(b). The uniform stress in the matrix indicates all matrix is yielded. In addition, after multiplication of a scale factor of 17.5, the expanding deformation of inclusion can be seen (brown color region, compared to the undeformed region indicated by a ¼ circle curve of the radius of 0.3). We remark that in all of our calculations deformation is assumed to be infinitesimal. Since the outer rim is fixed, the disc cannot expand freely, hence stress arises from thermal expansion of each phase, as well as the expanding competition between the inclusion and matrix. In addition, from (a), all curves do not show numerical oscillation, indicating the plane strain problem has superior numerical stability, as oppose to the plane stress problem discussed in the next section.

3.3 Two-dimensional analysis–plane stress

With all parameters that are the same as the plane strain case discussed in the previous section, the plane stress results are shown in Figs. 4 (a) and (b) for the von Mises stress under various

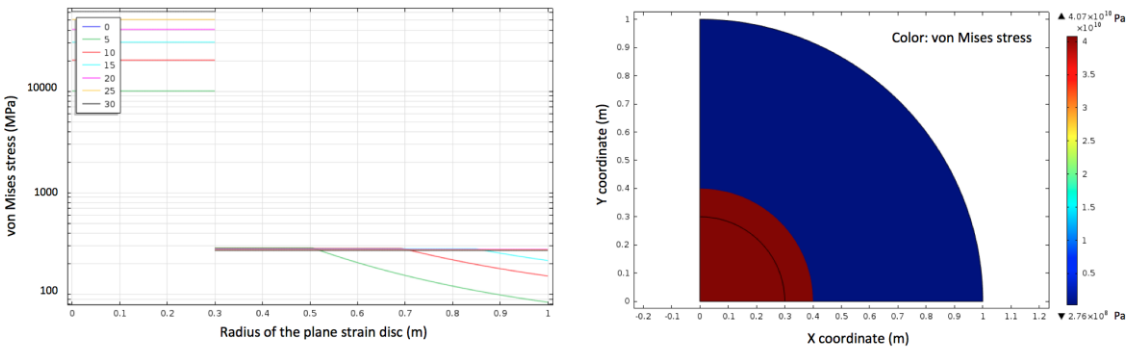

(a) Mises stress vs. radial position (b) Mises stress contour and deformation at ΔT=20℃

Fig. 3 Results from the plane strain composite disc

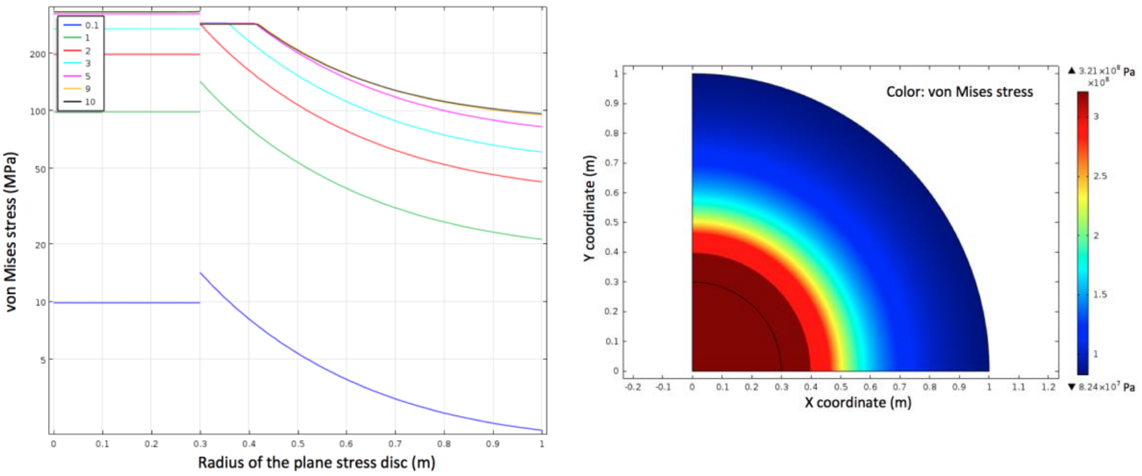

(a) Mises stress vs. radius (b) Mises stress contour and deformation at ΔT=5℃

Fig. 4 Results from the plane stress composite disc

temperature loading and its spatial distribution, respectively. The expanding deformation of the inclusion was multiplied with a scale factor of 67.4. The elastic irreversible temperature ΔT_e of the disc is determined to be about 2℃, determined by finer parametric analysis (not shown in the figure). Due to numerical difficulties, as discussed by Jetteur (1986), Kleiber and Kowalczyk (1996), the global plastic collapse of the plane stress temperature ΔT_p cannot be accurately determined. Our numerical results show ΔT_p is greater than 10℃; this can be viewed as a lower bound. The numerical difficulties can also be observed from the small changes in the plastic zone in the matrix between ΔT=9℃ and ΔT=10℃. Therefore, it is strongly needed to have analytical solutions for the plane stress problem for benchmark testing on numerical results.

3.4 Three-dimensional analysis–long cylinder

It is known that long cylinder can be modeled as the plane strain disc for the cross section of the cylinder not close to its ends. Indeed, when using the 3D cylinder model to calculate the λ=10 case, we obtain the identical results as shown in Fig. 3(a), hence not repeatedly reported here. The fixed boundary condition used in the 3D cylinder case is consistent with the fixed boundary condition in the plane-strain case, hence their results are consistent. When λ=0.1, i.e., E_i/E_0=0.21 and γ_i/γ_0=0.43, the von Mises stress of the cylinder at its middle cross section (i.e., z=5 m cross section) is shown in Fig. 5. Since $E_i<E_0$, the inclusion is an elastically softer phase than the matrix at the reference temperature. By calculating the temperature loading ΔT up to 200℃ and monitoring the stress distribution along the radius in the cross section, as shown in Fig. 3(a), the elastic irreversible temperature ΔT_e and global plastic collapse temperature ΔT_p can be identified to be about 50 and 180℃, respectively. These values are significantly larger than the values reported in the previous sections for the plane problems due to different λ. The spatial distribution of the von Mises distribution in the cylinder when ΔT=100℃ is shown in Fig. 5(b) with color in units of Pa. We remark that when inclusion has smaller Young's modulus and thermal expansion coefficient than those of the matrix, the radius of the inclusion would become smaller than that of

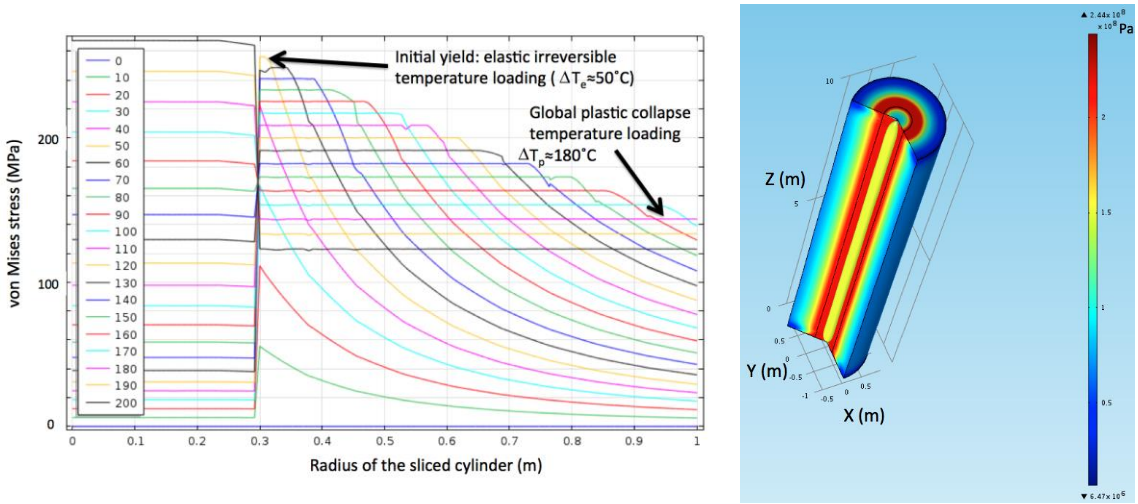

(a) von Mises stress vs. radial position on the middle cross section (b) von Mises stress distribution and deformation at ΔT=100℃

Fig. 5 Results from the 3D cylinder with axisymmetric assumption

the undeformed state under uniform heating. Global plastic collapse temperature can be easily calculated by the methodology presented here no matter the inclusion is an elastically hard or soft phase. Furthermore, the plane strain and 3D cylinder modeling would give rise to similar results.

3.5 Three-dimensional analysis – thin disc

With all parameters are the same as the 3D cylinder case, Fig. 6 shows the results of the 3D disc case with λ=10, same as the previous plane problems studied. The von Mises stress at the middle plane, i.e., height z=0.05 m, half of the thickness, is plotted against radius in Fig. 6(a). Due to large deformation around the inclusion-matrix interface, numerical calculations failed to find converged solutions after ΔT = 16℃ in the 3D disc case. The global plastic collapse temperature was not able to be determined, and ΔT=16℃ can be considered as its lower bound. The elastic irreversible temperature in the 3D disc case was found to be similar to that found in the plane stress problem, i.e., ΔT_e~2℃. In Fig. 6 (b), the expanding deformation of the inclusion can be seen after magnified with a scale factor of 22.8.

When λ=1 (E_i/E_0=2.1 and γ_i/γ_0=4.3), Fig. 7 shows the results of the 3D disc case, i.e., three-dimensional thin plate. The inclusion is a mildly elastically harder phase. From the von Mises stress distribution along the radius at various temperature loading, as shown in Fig. 6(a), the elastic irreversible temperature and global plastic collapse temperature are about 30℃ and 60℃, respectively. The spatial distribution of the von Mises distribution in the 3D disc when ΔT=30℃ is shown in Fig. 6(b), and its deformation is magnified for better viewing with a scale factor of 395. In addition to global plastic collapse, one may define a local plastic collapse due to significant stress variations near the inclusion-matrix interface. The need of introducing the concept of local plastic collapse is for 2D plane stress analysis since it cannot model the pile up, along the Z direction, phenomenon near the interface. As can be seen in Fig. 6(b), under the thermal loading, the disc expands along the Z direction, i.e., thickness direction, significantly from the

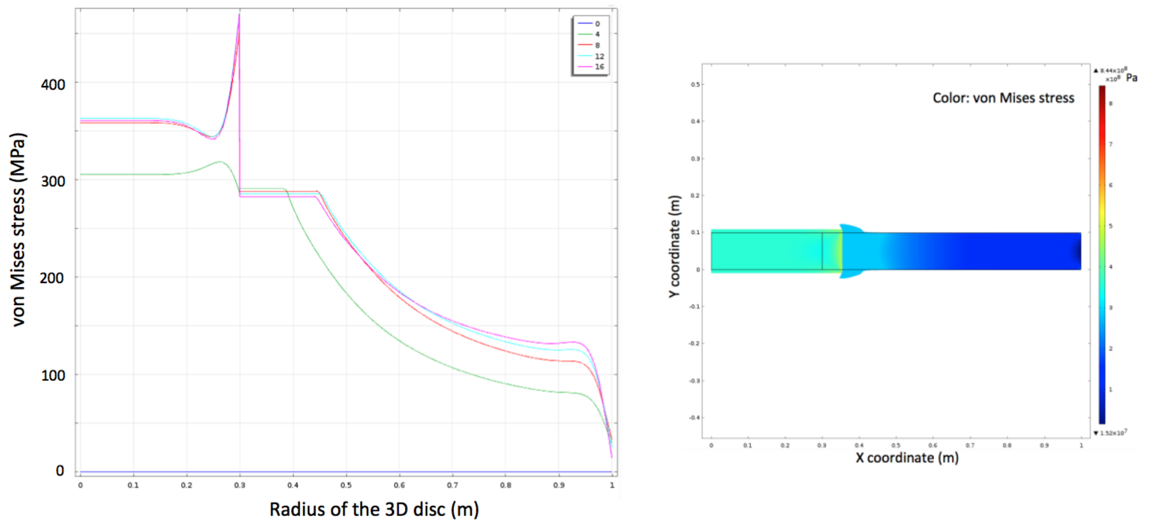

(a) von Mises stress vs. radial position at middle plane of the plate

(b) von Mises stress and deformation at ΔT=16℃

Fig. 6 Three-dimensional thin disc model with the axisymmetric assumption for λ=10.

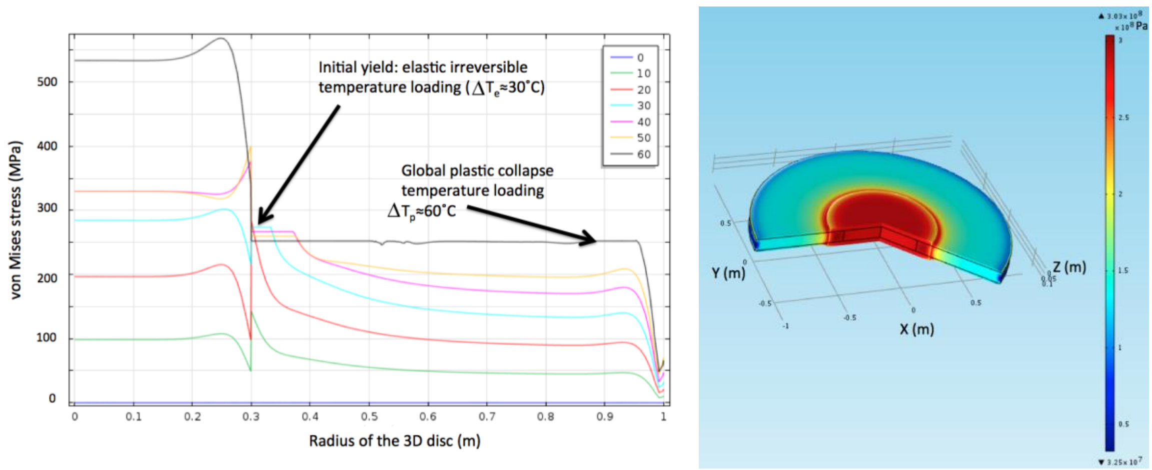

(a) von Mises stress vs. radial position at middle plane of the plate

(b) von Mises stress and deformation at ΔT=30℃

Fig. 7 Three-dimensional thin disc model with the axisymmetric assumption for λ=1

axisymmetric analysis. Therefore, in the 2D analysis, significant pile up may set a limitation on the validity of the analytical solutions of the plane stress problem, as a result of local plastic collapse. The principle stress distributions of the 3D disc with λ=1 are shown in Fig. 8 for the thermal loading ΔT_p=60℃, the global plastic collapse temperature. The principle stresses are more heterogeneous distributed near the inclusion-matrix interface.

To further examine the effects of λ, defined as $\lambda=E_i/E_{i0}=\gamma_i/\gamma_{i0}$, Figs. 9 (a) and (b) show the von Mises stress distribution along the radius for λ=0.1 and λ=0.01, respectively. The inclusions are an

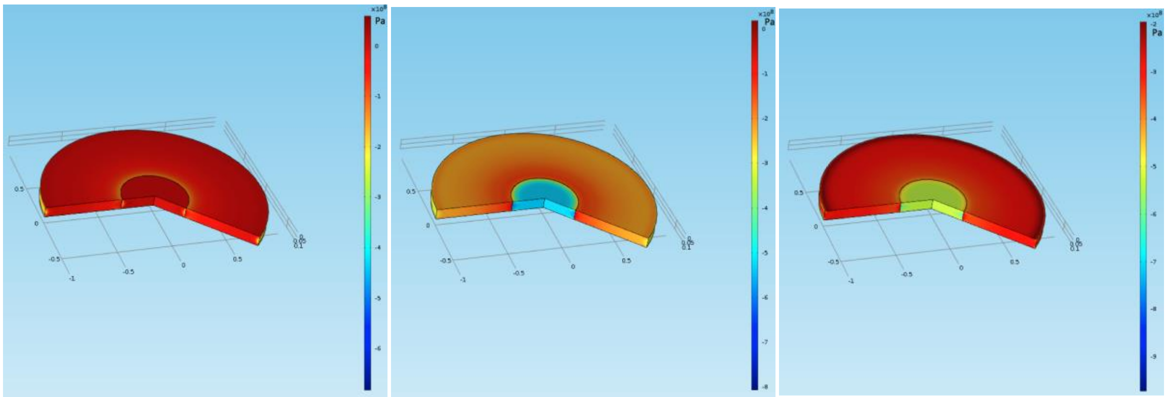

(a) First principle stress (b) Second principle stress (c) Third principle stress

Fig. 8 Principle stresses of the 3D disc with λ=1

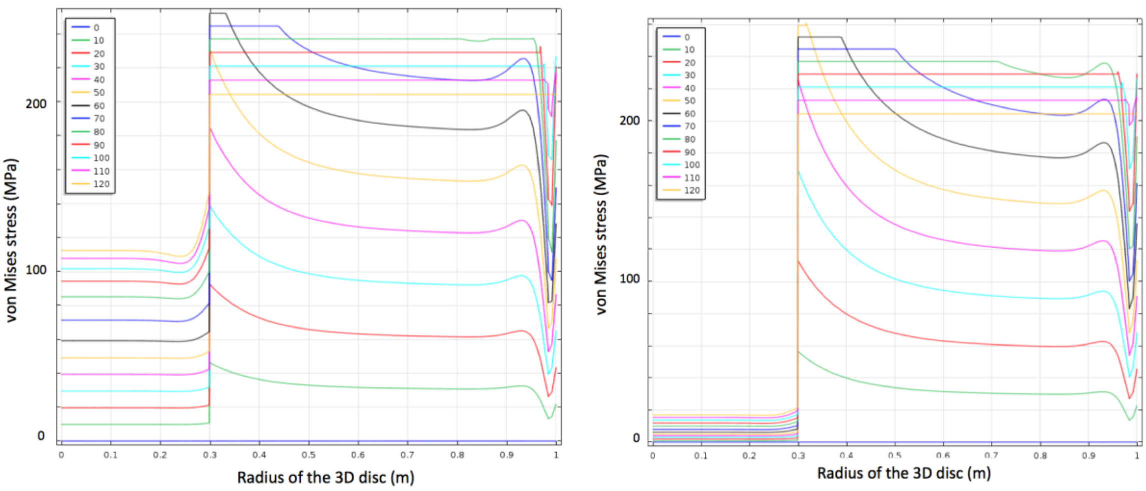

(a) for λ=0.1 (b) for λ=0.01

Fig. 9 Three-dimensional thin disc model with the axisymmetric assumption

elastically weaker phase. When decreasing λ, one reduces the Young's modulus and thermal expansion coefficient of the inclusion, hence the mechanical and thermal resistance from inclusion becomes weaker. When λ=0.1, ΔT_e=50~60℃ and ΔT_p=70~80℃. When λ=0.01, ΔT_e=40~50℃ and ΔT_p~80℃. The level of the stresses in the matrix of the two λ cases is similar, but very different in the inclusion due to its weakness. Therefore, weak inclusions play a minor role in the stress distribution in the matrix. In addition, for all three λ cases studied here, there is a significant stress drop near the outer rim of the 3D disc, which is not seen in the plane stress results. Since, in the 3D disc, only the circumferential surface on the outer rim is fixed, the effective stress may be strongly affected by the local deformation along the Z direction (thickness direction). The strange tail behaviour in the von Mises stress vs. radius plot is due to the fixed boundary condition used in the 3D disc is different from that in the plane stress case. In the 3D disc, the fixed boundary condition on the outer rim sets zero displacement along the three orthogonal coordinates, while in

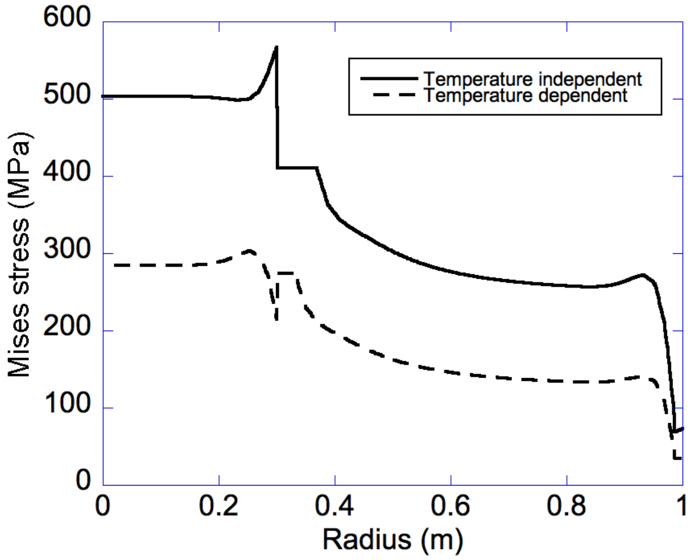

Fig. 10 Effects of temperature-dependent material properties for the 3D disc with λ=1 and ΔT=40 ℃

the plane stress, only the two in-plane displacements are set to be zero.

With the chosen parameters used in the finite element calculations for λ=1, Fig. 10 shows the Mises stress distribution along the radius for the temperature-dependent and temperature-independent material properties under a given temperature difference loading (ΔT=40℃). Since the yield stress in the temperature dependent case is largely reduced at high temperature, the Mises stress is expected to be smaller than that for the temperature independent case. In other words, analysis based on the temperature independent model always overestimates the capacity of the materials, which leads to non-conservative design. We remark that, in Figs. 6-10, von Mises stress distribution showing a strange behavior near the outer rim of the disc is due to the fixed boundary condition that set zero displacements along three orthogonal coordinates. The deformation near the outer rim is not uniform along the z axis under the fixed boundary condition in the 3D disc case.

4. Conclusions

Based on our numerical results from the composite disc, when material and geometric parameters are chosen to be the same, the plane and 3D solutions show similar results in terms of von Mises stress distribution, elastic-irreversible temperature and plastic collapse temperature. In our 3D disc case, von Mises stress distribution is significantly different from the plane stress case because of the fixed boundary condition setting zero displacement along the three coordinates. For the elastically hard inclusion, the plane stress and 3D disc case may encounter numerical difficulties due to local plastic collapse, i.e., large deformation, at the inclusion-matrix interface. Since the plane stress assumption does not consider stress in the z direction, it may not be able to correctly model the composite disc when pile up is significant. In addition, considerations of temperature-dependent mechanical properties are crucial to obtain realistic results when under temperature loading.

Acknowledgments

Funding from Taiwan Ministry of Science and Technology and Russian Foundation for Basic Research under the contract number of NSC 103-2923-E-006-003-MY3 and RFBR-14-08-92003 for the Taiwan-Russia bilateral collaboration project is gratefully appreciated. This research was, in part, supported by the Ministry of Education, Taiwan, R.O.C. The Aim for the Top University Project to the National Cheng Kung University (NCKU). We are grateful to the National Center for High-performance Computing for computer time and facilities.

References

Alexandrov, S. and Alexandrova, N. (2001), “Thermal effects on the development of plastic zones in thin axisymmetric plates”, *J. Strain Anal. Eng. Des.*, **36**, 169-175.

Alexandrov, S. and Chikanova, N. (2000), “Elastic-plastic stress-strain state of a plate with a pressed-in inclusion in thermal field”, *Mech. Solid.*, **35**, 125-132.

Alexandrov, S.E., Lomakin, E.V. and Jeng, Y.R. (2012), “Solution of the thermoelasticplastic problem for a thin disk of plastically compressible material subject to thermal loading”, *Dokl. Phys.*, **57**, 136-139.

Alexandrov, S., Wang, Y.C. and Aizikovich, S. (2014), “Effect of temperature-dependent mechanical properties on plastic collapse of thin discs”, *J. Mech. Eng. Sci. Part C*, **228**(14), 2483-2487.

Alexandrov, S., Wang, Y.C. and Jeng, Y.R. (2014), “Elastic-plastic stresses and strains in thin discs with temperature-dependent properties subject to thermal loading”, *J. Therm. Stress.*, **37**, 488-505.

Altan, G., Topcu, M., Bektas, N.B. and Altan, B.D. (2008), “Elastic-plastic thermal stress analysis of an aluminum composite disc under parabolic thermal load distribution”, *J. Mech. Sci. Technol.*, **22**, 2318-2327.

Argeso, H. and Eraslan, A.N. (2008), “On the use of temperature-dependent physical properties in thermomechanical calculations for solid and hollow cylinders”, *Int. J. Therm. Sci.*, **47**, 136-146.

Ball, D.L. (1995), “Elastic-plastic stress analysis of cold expanded fastener holes”, *Fat. Fract. Eng. Mater. Struct.*, **18**, 47-63.

Bengeri, M. and Mack, W. (1994), “The influence of the temperature dependence of the yield stress on the stress distribution in a thermally assembled elastic-plastic shrink fit”, *Acta Mech.*, **103**, 243-257.

COMSOL website (2015), www.comsol.com.

Eraslan, A.N. and Akis, T. (2003), “On the elastic-plastic deformation of a rotating disk subjected to radial temperature gradient”, *Mech. Bas. Des. Struct. Mach.*, **31**, 529-561.

Eshelby, J.D. (1957), “The determination of the elastic field of an ellipsoidal inclusion and related problems”, *Proc. R. Soc. Lond. A*, **241**, 1376-1396.

Guven, U. (1997), “The fully plastic rotating disk with rigid inclusion”, *ZAMM*, **77**(9), 714-716.

Guven, U. and Altay, O. (1998), “Linear hardening solid disk with rigid casing subjected to a uniform heat source”, *Mech. Res. Commun.*, **25**, 679-684.

Jetteur, P. (1986), “Implicit integration algorithm for elastoplasticity in plane strain analysis”, *Eng. Comp.*, **3**, 251-253.

Kleiber, M. and Kowalczyk, P. (1996), “Sensitivity analysis in plane stress elasto-plasticity and elasto-viscoplasticity”, *Comp. Meth. Appl. Mech. Eng.*, **137**, 395-409.

Krenev, L.I., Aizikovich, S.M., Tokovyy, Y.V. and Wang, Y.C. (2015), “Axisymmetric problem on the indentation of a hot circular punch into an arbitrarily nonhomogeneous half-space”, *Int. J. Solid. Struct.*, **59**, 18-28.

Kwon, P., Dharan, C.K.H. and Ferrari, M. (1994), “Macroscopic analysis of axisymmetric functionally gradient materials under thermal loading”, *ASME J. Energy Res. Tech.*, **116**, 115-120.

Lubliner, J. (1990), *Plasticity Theory*, Macmillan Publishing Company, New York.

Luxmoore, A.R., Light, M.F. and Evans, W.T. (1977), "A comparison of finite-element and experimental studies on plane stress crack geometries", *J. Strain Anal. Eng. Des.*, **12**, 208-216.
Lutz, M.P. and Zimmerman, R.W. (1996), "Thermal stresses and effective thermal expansion coefficient of a functionally gradient sphere", *J. Therm. Stress.*, **19**, 39-54.
Mack, W. and Bengeri, M. (1994), "Thermal assembly of an elastic-plastic shrink fit with solid inclusion", *Int. J. Mech. Sci.*, **36**, 699-705.
Mack, W. and Plochl, M. (2000), "Transient heating of a rotating elastic-plastic shrink fit", *Int. J. Eng. Sci.* **38**, 921-938.
Noda, N. (1991), "Thermal stresses in materials with temperature-dependent properties", *Appl. Mech. Rev.*, **44**, 383-397.
Parmaksizoglu, C. and Guven, U. (1998), "Plastic stress distribution in a rotating disk with rigid inclusion under a radial temperature gradient", *Mech. Struct. Mach.*, **26**, 9-20.
Reddy, J.N., Chin, C.D. (1998). "Thermomechanical analysis of functionally graded cylinders and plates", *J. Therm. Stress.*, **21**, 593-626.
Sayman, O. and Arman, Y. (2006), "Thermal stresses in a thermoplastic composite disc under a steady state temperature distribution", *J. Rein. Plast. Comp.*, **25**, 1709-1722.
Simo, J.C. and Taylor, R.L. (1986), "A return mapping algorithm for plane stress elastoplasticity", *Int. J. Numer. Meth. Eng.*, **22**, 649-670.
Topcu, M., Altan, G., Callioglu, H. and Altan, B.D. (2008), "Thermal elastic-plastic analysis of an aluminium composite disc under linearly decreasing thermal loading", *Adv. Comp. Lett.*, **17**, 87-96.
Triantafyllou, S.P. and Koumousis, V.K. (2012), "An hysteretic quadrilateral plane stress element", *Arch. Appl. Mech.*, **82**, 1675-1687.
Valoroso, N., Rosati, L. (2009), "Consistent derivation of the constitutive algorithm for plane stress isotropic plasticity. part I: theoretical formulation", *Int. J. Solid. Struct.*, **46**, 74-91.
Wang, Y.C., Alexandrov, S. and Jeng, Y.R. (2013), "Effects of thickness variations on the thermal elastoplastic behavior of annular discs", *Struct. Eng. Mech.*, **47**(6), 839-856.
Wang, Y.C. and Ko, C.C. (2015), "Energy dissipation of steel-polymer composite beam-column connector", *Steel Compos. Struct.*, **18**(5), 1161-1176.